Human p53 Is Inhibited by Glutathionylation of Cysteines Present in the Proximal DNA-Binding Domain during Oxidative Stress[†,‡]

Chinavenmeni S. Velu,[§] Suryakant K. Niture,[§] Catalin E. Doneanu,[||] Nagarajan Pattabiraman,[⊥] and Kalkunte S. Srivenugopal*[,§]

Anticancer Resistance Research Group, Department of Pharmaceutical Sciences, Texas Tech University Health Sciences Center, Amarillo, Texas 79106, Mass Spectrometry Center, Department of Medicinal Chemistry, University of Washington, Seattle, Washington 98195, and Department of Oncology, Lombardi Comprehensive Cancer Center, Georgetown University, Washington, D.C. 20057

Received March 2, 2007; Revised Manuscript Received April 23, 2007

ABSTRACT: The cellular mechanisms that modulate the redox state of p53 tumor suppressor remain unclear, although its DNA binding function is known to be strongly inhibited by oxidative and nitrosative stresses. We show that human p53 is subjected to a new and reversible posttranslational modification, namely, S-glutathionylation in stressed states, including DNA damage. First, a rapid and direct incorporation of biotinylated GSH or GSSG into the purified recombinant p53 protein was observed. The modified p53 had a significantly weakened ability to bind its consensus DNA sequence. Reciprocal immunoprecipitations and a GST overlay assay showed that p53 in tumor cells was marginally glutathionylated; however, the level of modification increased greatly after oxidant and DNA-damaging treatments. GSH modification coexisted with the serine phophorylations in activated p53, and the thiol-conjugated protein was present in nuclei. When tumor cells treated with camptothecin or cisplatin were subsequently exposed to glutathione-enhancing agents, p53 underwent dethiolation accompanied by detectable increases in the level of $p21^{waf1}$ expression, relative to the DNA-damaging drugs alone. Mass spectrometry of GSH-modified p53 protein identified cysteines 124, 141, and 182, all present in the proximal DNA-binding domain, as the sites of glutathionylation. Biotinylated maleimide also reacted rapidly with Cys141, implying that this is the most reactive cysteine on the p53 surface. The glutathionylatable cysteines were found to exist in a negatively charged microenvironment in cellular p53. Molecular modeling studies located Cys124 and -141 at the dimer interface of p53 and showed glutathionylation of either residue would inhibit p53−DNA association and also interfere with protein dimerization. These results show for the first time that shielding of reactive cysteines contributes to a negative regulation for human p53 and imply that such an inactivation of the transcription factor may represent an acute defensive response with significant consequences for oncogenesis.

The p53 gene product is a DNA sequence-specific transcription factor, which as a homotetramer controls the expression of a wide array of genes through direct binding with response elements (*1*). This best studied and probably most important function bestows human p53 with regulatory responses to a variety of cellular stresses, including DNA damage, nucleotide depletion, chemotherapeutic drugs, oxidative stress, and many aberrant growth signals (*2*, *3*). A complex and diverse set of posttranslational modifications, such as the site-specific phosphorylations, ubiquitination, and sumoylation, govern the activation and stabilization of the p53 protein in these functional transactions (*4*). However, the cellular mechanisms including covalent modifications, if any, that protect and modulate the p53 protein during the constant and recurring episodes of oxidative and nitrosoative stresses, which often initiate and promote carcinogenesis and many disease states (*5*), remain unknown. Several lines of evidence suggest that p53 is highly prone to oxidative inactivation. For example, the in vitro binding of p53 to its recognition sequences requires the presence of a reductant such as 2-mercaptoethanol or dithiothreitol in the binding

[†] This work was supported by grants from the National Institutes of Health (RO1 CA97343) and the Women's Health Research Institute of Amarillo to K.S.S.

[‡] Part of this study was presented at the 97th annual meeting of the American Association for Cancer Research, Washington, DC, April 1−5, 2006.

* To whom correspondence should be addressed: Department of Pharmaceutical Sciences, Texas Tech University Health Sciences Center, 1400 Wallace Blvd., Amarillo, TX 79106. Telephone: (806) 356-4660,ext.221.Fax: (806)356-4663.E-mail: kalkunte.srivenugopal@ttuhsc.edu.

[§] Texas Tech University Health Sciences Center.

[||] University of Washington.

[⊥] Georgetown University.

[1] Abbreviations: Biot-GSH, biotinylated glutathione; Biot-GSSG, biotinylated glutathione disulfide; Biot-GST, biotinylated glutathione *S*-transferase; CID, collision-induced dissociation; Cispt, cisplatin; CPT, camptothecin; DA, diamide; DAE/NO, 2,2-diethyl-1-nitrosooxyhydrazine sodium salt; DAI, DNA affinity immunoblotting; DBD, DNA-binding domain; DTT, dithiothreitol; ECL, enhanced chemiluminescence; EMSA, electrophoretic mobility shift assay; ESI, electrospray ionization; GEE, glutathione monoethyl ester; IP, immunoprecipitation; MALDI, matrix-assisted laser desorption ionization; NAC, *N*-acetyl-L-cysteine; NEM, *N*-ethylmaleimide; rp53, human recombinant p53 protein; Strep-HRP, streptavidin-linked horseradish peroxidase; TBH, *tert*-butyl hydroperoxide; TOF, time-of-flight; WB, Western blot.

10.1021/bi700425y CCC: $37.00
Published on Web 06/08/2007

buffers and is sensitive to oxidants such as H_2O_2 and diamide (*6*). Target gene transactivation by p53 in human cells is affected by the pharmacological oxidizing and reducing agents (*7*). The level of expression of reporter genes driven by a p53-responsive promoter is also decreased by oxidative treatment (*8*). Hypoxia and nitric oxide-induced inactivation of p53-dependent transactivation are yet other examples (*9*, *10*). The transactions of p53 are also sensitive to metal cations and Cu^{2+}/Cu^{+} redox cycling (*11*). In contrast to the oxidation effects, the Ref-1 and thioredoxin redox modulators have been shown to reactivate oxidized p53 and stimulate p53 transactivation in cells (*12*, *13*). Therefore, p53 resembles other redox-dependent transcription factors such as NF-κB and AP-1 in these properties.

A majority of the redox-sensitive proteins contain one or more cysteines that exist as thiolate anions, also called reactive cysteines, which play crucial roles in redox signaling (*14*). The reactive cysteines are more nucleophilic and, therefore, are highly sensitive to attack by reactive oxygen and reactive nitrogen species (ROS and RNS, respectively) (*15*). ROS and RNS cause oxidation of protein thiols (PSH) in a stepwise fashion involving the formation of thiyl radical ($PS^{\bullet}$), sulfenic acid (PSOH), sulfinic acid (PSO_2H), sulfonic acid (PSO_3H), or S-nitrosothiol/S-nitrosated proteins (PSNO). All these forms except PSO_3H can be stabilized within the protein environment and recycled, via disulfide bond intermediates, back to the thiol state (*16*). In this process called S-thiolation, low-molecular weight thiols such as glutathione (GSH or GSSG) can form mixed disulfides with reactive cysteines or oxidized cysteine forms in proteins (*17*). This modification is readily reversible, because increases in the GSH:GSSG ratio or enzymatic reactions involving protein disulfide isomerase, glutaredoxin, thioredoxin, or sulfiredoxin can restore the protein sulfhydryls to their reduced state (*18*). Thus, glutathionylation of reactive cysteines in metabolic enzymes, kinases, phosphatases, and transcription factors has emerged as a central mechanism by which changes in the intracellular redox state may be transduced into functional cellular responses (*18*). Very much like phosphorylation, this modification can modulate enzyme activities, protein functions, and protein−protein interactions (*17*, *18*).

Pertinent to this study, evidence of the involvement of cysteines in the redox modulation and DNA binding function of p53 has been discovered (*19*−*22*). Human p53 protein has 10 cysteine residues, all of which, interestingly, are located within the DNA-binding domain (DBD),[1] between amino acids 100 and 300 (*19*). The positions of cysteines relative to the recognition loop in the tertiary structure of p53 are shown in Figure S1 of the Supporting Information. Cysteines 176, 238, and 242 along with histidine 179 bind to a divalent zinc atom, which stabilizes the loop and helical structure of the core domain. Mutagenesis of these cysteines leads to a complete loss of DNA binding, while replacement of cysteines 124, 135, 141, and 277 alters the affinity of murine p53 for DNA, suggesting that the latter group of cysteines may regulate the structural dynamics of DBD (*19*, *21*). Nevertheless, which of these cysteines are most reactive and respond to oxidative insults in human cells is not known. Also, the consequences of these responses, if any, to p53 function and cell signaling remain unclear. In this report, we show that human p53 is a substrate for glutathionylation in vitro and in cells and demonstrate the site-specific modification of three cysteines present in the proximal core domain disrupts the interaction of p53 with its target DNA. Evidence of the modulation of p53 function by glutathionylation in cells is also presented.

MATERIALS AND METHODS

Cell Lines and Reagents. Human cancer cell lines, U87 malignant glioblastoma (U87MG) and HCT116 colon carcinoma, both of which harbor a wild-type p53 (*23*), were used. Most reagents, of the highest available grade, were obtained from Sigma Chemicals. Monoclonal antibodies to p53 (DO-1) and glutathione were purchased from Santa Cruz Biotechnology and Virogen, respectively.

Expression and Purification of Recombinant p53 Protein (rp3). The *Escherichia coli* BL21(DE3) strain was transformed with a pRSET plasmid containing histidine-tagged wild-type human p53 coding sequence (*24*) kindly provided by J. Nyborg (Colorado State University, Fort Collins, CO). Protein expression was initiated by the addition of inducer (an IPTG alternative from MoleculA), which provided more soluble protein. rp53 in its native form was purified by metal chelation chromatography on Talon resin (BD Biosciences) as described previously (*25*). Dialyzed protein (90% homogeneity) was stored frozen in the presence of 25 μM β-mercaptoethanol. For glutathionylation studies described in this report, the protein preparations were dialyzed against 50 mM Tris-HCl (pH 8.0) at 4 °C immediately before being used.

Biotinylation of GSH, GSSG, and GST-pi Protein and Their Use for Detection of Glutathionylated p53. Biotinylation of GSH and GSSG was performed according to the method of Sullivan et al. (*26*) using sulfo-NSH-biotin (Pierce Biochemicals). Human placental glutathione *S*-transferase protein (GST-pi) was biotinylated for detection of glutathionylated p53 by the overlay assays as described previously (*27*). For this, purified GST-pi (0.5 mg) was immobilized on GSH-Sepharose to protect the GSH-binding site, and the bound protein was treated with sulfo-NSH-biotin. The beads were washed, and biotinylated GST was eluted with 10 mM GSH followed by dialysis (*27*). After incubation of rp53 (0.5 μg) with 5 mM biotinylated thiols (Biot-GSH and Biot-GSSG) in phosphate buffer (pH 7.5), 10 mM *N*-ethylmaleimide (NEM) was added to stop the reactions. The samples were assessed by nonreducing SDS−PAGE, and proteins were transferred to PVDF membranes. The blots were soaked in 5% nonfat dry milk and incubated with streptavidin-linked HRP (Pierce, 1:8000 dilution), followed by washings and enhanced chemiluminescence (ECL). The biotinylated GST protein retains the ability to bind the glutathione moiety present in the mixed disulfide linkages formed by glutathionylation (*27*−*29*); a Far-western procedure described previously (*27*) was used for detecting GSH-linked p53. Briefly, the p53 protein was immunoprecipitated from control and drug-treated cells, and the complexes were resolved by nonreducing SDS−PAGE followed by protein blotting. Next, the membranes were blocked with 5% BSA and incubated with biotinylated GST-pi (30 μg/mL) for 10 h. After extensive washings, the blots were exposed to streptavidin-bound HRP (Strep-HRP) followed by ECL (*27*).

Combined Immunoprecipitation Immunoblotting Analysis. For immunoprecipitation of the glutathione-conjugated p53

protein, tumor cells were lysed at 4 °C in Tris-buffered saline containing 1× protease cocktail (Sigma), 0.5 mM sodium vanadate, and 0.5% NP-40 as described previously (*25*). Equal protein amounts in lysates from different treatments were precleaned with 5 μL of protein A−agarose beads, and the proteins were immunoprecipitated using monoclonal antibodies to p53 or GSH. The complexes were solubilized in nonreducing SDS sample buffers and subjected to electrophoresis on 10% gels followed by Western blot analysis using reciprocal antibodies.

Quantitation of p53 Binding with Target DNA by Affinity Immunoblotting (DAI) and Electrophoretic Mobility Shift Assays (EMSAs). Binding of p53 to its consensus recognition sequences was examined by the biotin-oligo pulldown assay followed by Western blotting (*30*). ds-5′-TAC AGA ACA TGT CTA AGC ATG CTG GGG ACT-3′ and mutant 5′-TAC AGA ATC GCT CTA AGC ATG CTG GGG ACT-3′ oligomers were labeled with biotin at the 5′ end on one strand (Integrated DNA Technologies). Equal amounts (1 μg) of unmodified and glutathionylated rp53 protein were allowed to bind with duplex DNA in a binding buffer [20 mM Tris-HCl (pH 7.2), 1 mM EDTA, 0.1% Triton X-100, 4% glycerol, 1 μg of poly(dI·dC), and 100 mM NaCl] at 4 °C for 30 min. The DNA-bound protein complexes were captured by the addition of 10 μL of streptavidin magnetic beads (Roche Diagnostics), washed three times with 1 M NaCl, eluted by boiling the beads in SDS sample buffer, and electrophoresed. After protein transfer, Western blot analysis for p53 was performed (*30*). For the EMSA, the p53 consensus and mutant oligonucleotides were end labeled using T4 polynucleotide kinase (New England Biolabs) and [γ-^{32}P]ATP in 10× kinase buffer supplied with the enzyme. p53 recombinant protein, treated with GSH or untreated, was preincubated in 5 μL of 5× binding buffer (20% glycerol, 5 mM $MgCl_2$, 5 mM EDTA, 5 mM dithiothreitol, 500 mM NaCl, 50 mM Tris-HCl, and 0.4 mg/mL calf thymus DNA) and 2 μg of poly(dI·dC) for 15 min followed by binding with labeled oligonucleotide for 30 min. Some samples were incubated with 200 ng of anti-p53 antibody before the addition of labeled probes. The proteins were separated by electrophoresis using a 4% native polyacrylamide gel and 40 mM Tris borate-EDTA (pH 7.5) as a running buffer. Gels were dried and exposed to Kodak X-ray film overnight.

Analysis of Glutathionylation Susceptibility of p53 Protein in Human Cancer Cells. Our recently published procedure regarding the ability of GSH-Sepharose to detect the redox changes in proteins (*31*) was applied. U87MG cells were treated with H_2O_2 (15 min exposure at 0.4 mM) and further postincubated in oxidant-free medium for 0.5−6 h. Extracts from these cells were prepared in PBS, and equal protein amounts therefrom were then mixed with 0.1 mL of GSH-Sepharose beads (*31*). The bound proteins were eluted with 10 mM DTT, resolved by SDS−PAGE, and Western blotted for p53.

Mass Spectrometry for Identification of Glutathionylation Sites on p53 Protein. In the first approach, rp53 samples (25 μg) treated with GSH (1 h at 37 °C) and untreated were resolved by SDS−PAGE. The protein bands in gel slices were digested with trypsin (25 ng/μL) in 25 mM NH_4HCO_3, and peptides were extracted and reconstituted with 0.1% formic acid (*32*). On-line nano-liquid chromatography and electrospray ionization mass spectrometry (nanoLC−ESI-MS/MS experiments) were performed on a QTOF API-US mass spectrometer (Micromass) equipped with the CapLC system (Waters, Milford, MA). The stream select module was configured with an OPTI-PAK Symmetry 300 C18 trap column (Waters) connected in series with a nanoscale analytical column. Peptide samples (5 μL) were injected onto the trap column, cleaned up, and back-flushed to the analytical column at a rate of 0.5 mL/min using gradient elution. The gradient consisted of 5−50% (v/v) solvent B containing 95% (v/v) acetonitrile and 0.1% (v/v) formic acid, over 45 min, followed by 50% B for 15 min and 50−90% B for 5 min [solvent A being 5% (v/v) acetonitrile and 0.1% (v/v) formic acid]. The MS/MS spectra recorded for the doubly and triply charged molecular ions of peptides were searched against the nonredundant National Center for Biotechnology Information protein database using the MASCOT search engine (*33*).

In the second method, rp53 protein was exposed to 5 mM biotinylated maleimide (Sigma Chemicals) for 5 min for rapid alkylation of surface thiol groups as described previously (*34*). The samples were immediately filtered on P6-Biogel spin columns for removal of the alkylator. The thiolated protein was trypsinized, and the peptides were allowed to bind with soft-link monomeric avidin resin (Promega) and washed with 0.15 M NaCl (*34*). The bound peptides were eluted with 10% acetic acid (200 μL) and analyzed by MALDI-TOF using an Autoflex II instrument (Bruker, Bremen, Germany) and by MALDI-TOF MS/MS (matrix-assisted laser desorption ionization time-of-flight tandem mass spectrometry) on a 4700 Proteomics Analyzer mass spectrometer (Applied Biosystems, Foster City, CA) in positive ion mode. The MALDI probe was spotted with 1 μL of a 1:1 (v/v) mixture of peptide sample and a saturated solution of α-cyano-4-hydroxycinnamic acid in 50% (v/v) acetonitrile. The conditions used for the operation of Autoflex II, acquisition of the data by MS/MS analysis, were the same as those described previously (*35*). The experimentally determined peptide fragment ion masses were matched, within a window of ±0.1 Da, to theoretical fragment ion masses generated by in silico fragmentation of p53 peptides.

Labeling of Cellular p53 by Biotinylated Maleimide. To demonstrate the rapid modification of reactive cysteines present on the p53 protein surface, cell free extracts were prepared in 40 mM Tris-HCl, 1 mM PMSF, 3 mM benzamidine, and 1 mM EDTA and dialyzed against the same buffer for 30 min. Three hundred microgram protein aliquots were exposed to 5 mM biot-maleimide, with and without 5 mM NEM treatment for 5−25 min. The samples were then subjected to immunoprecipitation of p53, and incorporation of the biotin group was detected by Western blot analysis using strep-HRP as described in an earlier section.

Nuclear Localization of Glutathionylated p53 Protein. Cytoplasmic and nuclear fractions from control and diamide-treated cells were separated using an extraction kit (Pierce Biochemicals) according to the manufacturer's instructions. Equivalent protein amounts from these fractions were immunoprecipitated using p53 antibodies. The immunocomplexes were run on SDS−polyacrylamide gels and Western blotted using anti-GSH antibodies.

Protein Modeling. The crystal structure of three p53 core regions consisting of amino acids 92−292 with a segment of DNA containing the consensus sequence (*36*) was obtained

from the Protein Data Bank (PDB entry 1TSR). Its three-dimensional image was visualized and manipulated using Sibyl 6.9 (Tripos Inc., St. Louis, MO). In this crystal structure, three p53 monomers (A, B, and C) are associated with a DNA duplex. Two of these (A and B) make direct contacts with the DNA. The third one (C) makes contact with the B monomer, but not with DNA (*36*). Therefore, the C chain was not included in this study. Also, Cys182 seen in the B chain faces away from the DNA duplex at the B−C dimer interface; therefore, glutathionylation of Cys182 was not studied here. The coordinates for glutathione were taken from the reported crystal structure of proteins containing covalently bound glutathione. Forty-one glutathione structures were obtained from the Protein Data Bank and analyzed for the conformations. We grouped the structures into two families of conformations: (1) extended and (2) folded. To simulate glutathionylation, we visually docked one conformation of each of the families of glutathione molecules and formed a covalent bond with either Cys124 or Cys141 of the p53 crystal structure. The coordinates of the whole complex were subjected to energy minimization using the CFF91 force field of the simulation program DISCOVER (Accelrys Inc., San Diego, CA). A distance-dependent dielectric constant was used in calculating the electrostatic energy. The coordinates for the DNA duplex were kept fixed during the minimization, and minimization was terminated when the root-mean-square value was less than 0.001 kcal/Å.

Statistical Analysis. All experiments, including the DNA binding assays for p53, IP/Western analysis, and mass spectroscopy procedures were performed at least three times in a manner independent of each other. Results were assessed by a Student's *t* test. Significance was defined as $p < 0.05$.

RESULTS

Direct Evidence for Incorporation of GSH and GSSG into p53 Protein. As a first step in characterizing p53 glutathionylation, we assayed the incorporation of GSH and GSSG into the accessible cysteines on the p53 surface. A rapid and time-dependent incorporation of Biot-GSSG (Figure 1A) or Biot-GSH (Figure 1B) was observed. Consistent with the thiol exchange mechanism, GSSG was more efficient than GSH with the initial burst of labeling observed at 5 and 20 min, respectively, in this reaction. The disulfide linkages thus induced are labile in the presence of reducing agents. In agreement, glutathionylation of rp53 was fully reversed when the modified protein was exposed to DTT before SDS−PAGE (Figure 1A,B). The blots exhibited equivalent p53 protein levels in all samples (bottom panels of Figure 1A,B), thus validating the assay and glutathionylation kinetics.

Decreased GSH:GSSG Ratios Promote S-Thiolation of p53. Protein glutathionylation is greatly enhanced by increased GSSG:GSH ratios that accompany cellular oxidative stress (*17*). Therefore, we examined incorporation of Biot-GSH into rp53 in the presence of varying GSH:GSSG ratios (100:1 to 0.1:1) that simulate mild to severe oxidative stress conditions in human cells. As shown in Figure 1C, glutathionylation of p53 occurred at very low GSSG concentrations, and it increased significantly at higher GSSG:GSH ratios (65% increase at a 1:1 ratio; bottom panel of Figure 1C), suggesting that p53 glutathionylation could occur in cells under physiological and moderately stressed conditions.

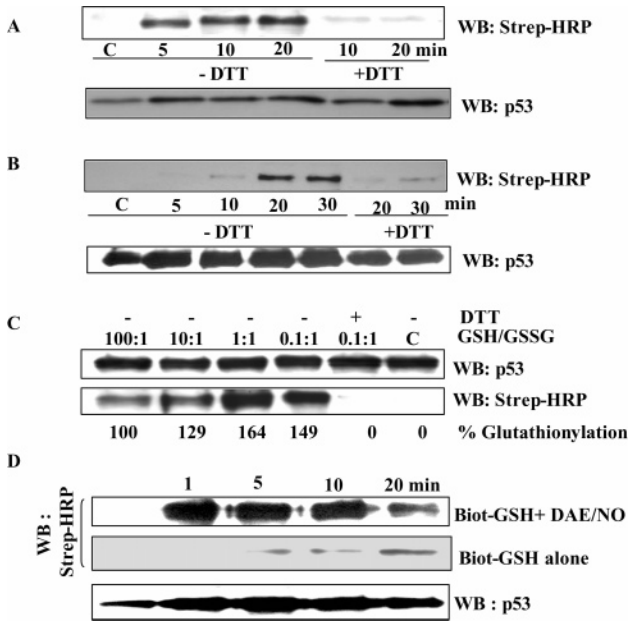

FIGURE 1: Human p53 protein is a substrate for glutathionylation in vitro. (A) Rapid incorporation of Biot-GSSG. rp53 (1 μg) was incubated with 5 mM Biot-GSSG in phosphate buffer at 37 °C for the indicated times. Some samples were mixed with 10 mM DTT before being loaded on nonreducing SDS−polyacrylamide gels. The blots were reacted with Strep-HRP to obtain the pattern shown. The kinetics of GSSG incorporation remained similar in three independent experiments ($p < 0.05$). Loading of p53 protein on these blots was assessed by Western analysis. (B) Kinetics of incorporation of Biot-GSH into rp53. rp53 was exposed to 5 mM Biot-GSH, and samples were processed as described in the legend of Figure 1A. (C) p53 glutathionylation is regulated by redox conditions. rp53 protein was treated with mixtures of GSH and GSSG (0.01−10 mM range) at different ratios in the presence of a constant amount of Biot-GSH (0.4 mM). The samples were incubated at 37 °C for 10 min, the reactions terminated with the addition of NEM, and the mixtures processed for blot analysis using Strep-HRP as described above. The bottom panel shows the results. DTT reversal of the glutathionylation is shown in lane 5. The blots were reprobed to assess p53 protein loading (top panel). (D) DAE/NO (NO-releasing agent) increases the level of p53 glutathionylation. rp53 was incubated with Biot-GSH in the presence or absence of 0.25 mM DAE/NO, and the labeling was assayed via the procedures described above.

Influence of Nitric Oxide on p53 Glutathionylation. While nitric oxide (NO) can modify the protein thiols directly by S-nitrosylation, it can also react with GSH to form GSNO which, in turn, can induce potent protein glutathionylation (*17*). Because the NO regulates p53 signaling (*10*, *37*), we exposed rp53 to Biot-GSH in the presence or absence of the NO donor (DEA/NO, 0.25 mM). Figure 1D shows that p53 was modified relatively faster and to a greater extent in the presence of NO donor, implying that nitrosative stress could induce glutathionylation of p53. This could occur through GSNO or the reaction of nitrosylated cysteines with GSH (*17*).

In Vitro Glutathionylation Inhibits Binding of p53 to the Recognition Sequence. Because cysteines modulate binding of p53 to DNA (*6*, *19*) and glutathionylation modifies the cysteines, we used a DNA affinity immunoblotting assay (DAI) to assess the binding of GSH-modified p53 to the biotinylated consensus or mutated recognition sequences (*30*). The DAI assay combines sensitive biotin/streptavidin affinity step and specific immunobloting to detect the DNA-bound p53 (*30*); therefore, this procedure was applied in most

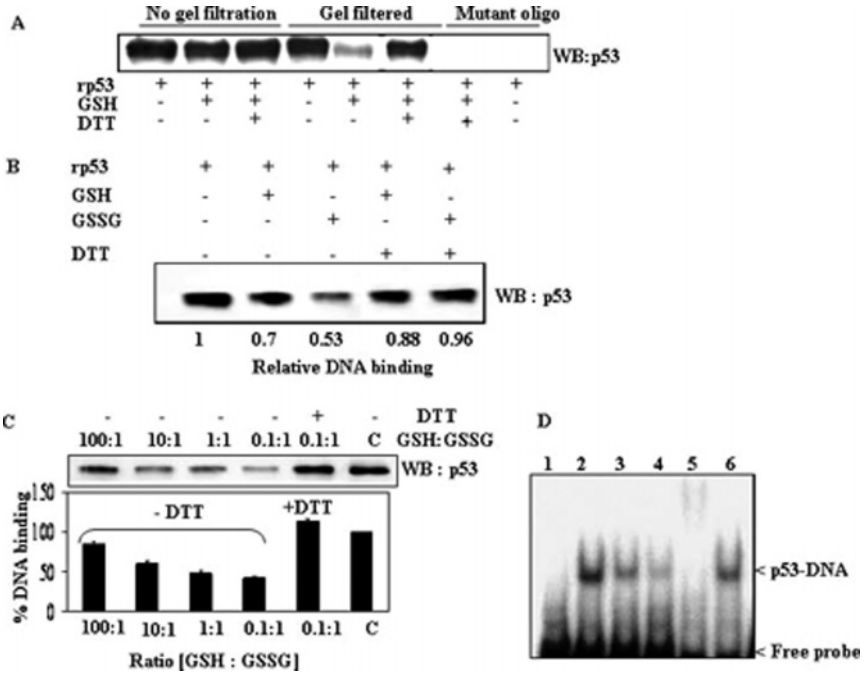

FIGURE 2: GSH or GSSG-modified p53 exhibits a significantly decreased level of binding to the consensus DNA sequence. (A) Reduction in the DNA binding activity of rp53 after GSH conjugation. The limited amounts of mercaptoethanol present in rp53 preparations were removed by brief dialysis and used for DNA binding studies described herein (see Materials and Methods). rp53 was incubated with and without GSH for 30 min. One set of samples (lanes 1−3) was subjected to a DNA affinity immunoblotting (DAI) assay without the GSH being removed (labeled no gel filtration). The other set was subjected to gel filtration on Bio-gel P6 spin columns prior to the binding. DAI was performed with biotinylated normal or mutant target sequences for p53. DNA-bound p53 levels are shown. (B) DNA binding assays of rp53 following glutathionylation with GSH or GSSG. rp53 protein at 0.5 μg was incubated with the thiols in sodium phosphate buffer (30 mM, pH 7.5), and all samples were then gel-filtered and DAI assays performed. In some samples, the gel-filtered protein was exposed to DTT before the addition of ds-target DNA. (C) rp53 was incubated with differing GSH:GSSG ratios (from 100:1 to 0.1:1) for 30 min. All samples were gel-filtered and DAI assays performed. Densitometry of the p53 bands was performed to calculate the percent DNA binding shown in the bar graph. Similar results were obtained in three separate experiments ($p < 0.05$). (D) Effect of glutathionylation on the EMSA of p53 binding to its recognition sequence. rp53 was incubated with GSH or GSSG followed by gel filtration as described above, and an EMSA was performed as described in Materials and Methods. Reaction mixtures in lanes 1−6 contained ^{32}P-labeled consensus recognition sequence: lane 1, untreated rp53 incubated with mutant oligo; lane 2, untreated rp53 incubated with consensus oligo; lane 3, rp53 incubated with GSH; lane 4, rp53 incubated with GSSG; lane 5, untreated rp53 incubated with p53 antibody (DO1) before addition of the probe to show supershift; and lane 6, rp53 incubated with GSSG, but treated with 5 mM DTT for 10 min prior to probe addition.

of our experiments. The Western blot in Figure 2A shows the results obtained in the initial assay. When rp53 was incubated with GSH for glutathionylation and DNA binding assays were performed without removing the thiol used for modification, no differences in the DNA binding of glutathionylated and nonglutathionylated p53 were apparent (compare lanes 1−3 in Figure 2A); rapid dethiolation by the excess of thiol present in the reaction mixtures may explain this observation. In contrast, when p53 samples were gel-filtered to remove GSH before DNA binding, a consistent and reproducible reduction in the level of binding of glutathionylated p53 to its target DNA was observed (compare lanes 4 and 5 in Figure 2A). As expected, exposure of the glutathionylated p53 to DTT restored the DNA binding to control levels (lane 6 in Figure 2A). In the next series, rp53 was glutathionylated in the presence of GSH or GSSG. The modified protein was purified by gel filtration, and DNA binding reactions were performed. The data in Figure 2B show that S-thiolation by both GSH and GSSG inhibited p53-specific DNA binding, GSSG was more efficient in this property, and treatment of the thiolated protein with DTT reversed the inhibition of DNA binding in all cases. Figure 2C depicts the DNA binding analysis of rp53 following glutathionylation at different GSH:GSSG ratios (from 100:1 to 0.1:1). The increased level of glutathionylation of p53 found under these oxidative stress simulating conditions (see Figure 1C) was clearly associated with weakened p53−DNA interactions. Overall, we observed a maximal reduction of 50% in p53 activity in glutathionylated samples.

Electrophoretic mobility shift assays (EMSAs) yielded similar data for binding of p53 to DNA. As shown in Figure 2D, the rp53 protein bound specifically to the consensus recognition sequence (lane 2) and exhibited a super shift in the presence of p53 antibodies (lane 5). GSH-treated (lane 3) and GSSG-treated (lane 4) p53 bound the DNA to a lesser extent, which was reversed by DTT (lane 6). Together, these results strongly suggest that changes in cellular redox inhibit p53 function through S-thiolation.

p53 Protein Is Glutathionylated in Human Tumor Cells. To demonstrate the p53 modification in cells, we used IP/Western blot analyses, a GST overlay assay (*27*), and GSH affinity chromatography for assessing glutathionylation susceptibility of the protein (*31*). First, for reciprocal IP/Western analyses, HCT116 colon cancer cells were treated with CPT to increase p53 levels, bulk glutathionylated proteins or p53 was immunoprecipitated using specific antibodies to GSH and p53, respectively, the IPs were electrophoresed on nonreducing SDS gels, and the resulting Western blots were probed with reciprocal antibodies. Figure 3A shows that p53 was detected among the proteins precipitated by anti-GSH antibodies, and p53 present in its IP was recognized by GSH antibodies. Exposing the IPs to

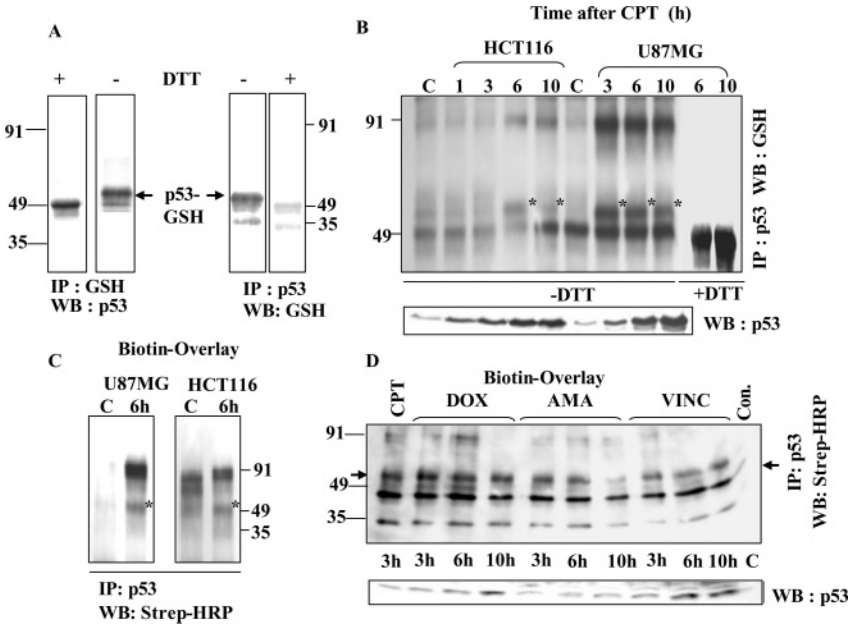

FIGURE 3: Detection of glutathionylated p53 protein in human tumor cells and its upregulation after DNA damage. (A) Evidence from reciprocal IP/Western analysis. HCT116 cells were treated with 25 μM CPT. Extracts (500 μg of protein) were immunoprecipitated using antibodies to p53 or GSH. The IPs were electrophoresed under nonreducing conditions and blotted, and reciprocal antibodies were used for p53 detection. Serial dilutions of the cell extracts followed p53 IP provided similar results (not shown). Wherever indicated, the immunoprecipitates were treated with 10 mM DTT for 10 min before SDS−PAGE. The DTT-treated sample exhibits a slightly faster migrating monomer in the left panel. GSH antibodies did not recognize p53 after DTT exposure in the right panel. (B) CPT-induced DNA damage is accompanied by a significant increase in levels of glutathionylated p53. HCT116 and U87MG cells were treated with 25 and 2.5 μM CPT, respectively. At each time point, p53 present in 500 μg protein samples was immunoprecipitated and processed for Western analysis using GSH antibodies. GSH-linked p53 bands are indicated with an asterisk. C stands for control. The immunoprecipitates in the last two lanes were treated with DTT before electrophoresis. The bottom panel represents a direct Western blot obtained after SDS−PAGE of cell extracts. (C) Detection of GSH-linked p53 by Biot-GST overlay. p53 IPs from control and 6 h CPT-treated U87MG and HCT116 cells were electrophoresed on nonreducing SDS gels and blotted. The membranes were incubated with Biot-GST protein followed by Strep-HRP staining as described in Materials and Methods. (D) Ability of anticancer drugs to generate glutathionylated p53 in U87MG cells. Cells were exposed to doxorubicin (DOX, 10 μM), amsacrine (AMA, 25 μM), and vincristine (VINC, 15 μM) for the indicated times. p53 present in the cell extracts (500 μg protein) was immunoprecipitated, and the resulting blots were subjected to a Biot-GST overlay assay, the results of which are shown in the top panel. The arrows on the left and right point to the position of the GSH-linked p53 band, which was not present in the untreated control (Con). The identity of bottom band is not known. The bottom panel shows the kinetics of p53 accumulation assessed by Western blot analysis of extracts from cells treated with the chemotherapy agents (DOX, AMA, and VINC).

DTT before SDS−PAGE slightly reduced the protein mass. These data clearly suggest that small amounts of p53 exist in a thiolated state in human cancer cells. Evidence from GST overlay assays and GSH affinity chromatography for this premise is presented in the sections to follow.

Ability of Anticancer Drugs To Induce Glutathionylation of p53. For testing the possibility of conjugation of p53 with GSH in the cellular response to DNA damage, the U87MG and HCT116 cells were treated with camptothecin (CPT) for the specified times, and p53 was immunoprecipitated. The Western blots generated therefrom were probed with antibodies to GSH. As expected, CPT increased the level of p53 expression in a time-dependent manner (direct Western blot shown in the bottom panel of Figure 3B). The top panel of Figure 3B shows that glutathionylated p53 (bands marked with an asterisk) appeared after DNA damage with different kinetics in the two cell lines. In HCT116 cells, marginal levels of GSH-modified p53 appeared 6 h after damage followed by its decline at 10 h; however, in U87MG cells, its levels were significantly higher at 3 and 6 h, followed by a decrease at 10 h. The 100 kDa protein band recognized by GSH antibodies appears to be p53 dimer, cross-linked by a disulfide bond. DTT treatment before PAGE led to the loss of the monomer and dimer protein bands, validating the specificity of the anti-GSH antibodies (last two lanes of Figure 3B). Far-Western analysis (overlay) using Biot-GST (*27*) was also used to verify the presence of GSH-conjugated p53 after DNA damage. For this, p53 immunocomplexes were electrophoresed and the resulting blots were incubated with Biot-GST protein, which retains the ability to bind protein-linked GSH residues (*27*); the protein-bound biotin groups were then detected by Strep-HRP staining. Figure 3C shows that in both U87MG and HCT116 cells, this method detected increased levels of glutathionylated p53 after DNA damage.

Many studies have shown that various anticancer drugs induce ROS, including oxygen free radicals, and cause oxidative stress (*38*). Therefore, we chose agents with these properties, namely, doxorubicin (DOX) and amsacrine (m-AMSA), which possess an anthracycline ring capable of quinone−semiquinone interconversions, and vincristine (VINC), a non-DNA binder, and analyzed kinetics of p53 thiolation in U87MG cells using the Biot-GST overlay. This method specifically detects the glutathionylated p53, but not the unmodified p53, relying on the recognition of GSH moieties present in the mixed disulfides by biotin-linked GST (*27*−*29*), and the subsequent detection of biotin groups in the sandwich by streptavidin-conjugated HRP. The data in Figure 3D reveal that while untreated control (far right lane) had no modified p53, the three anticancer drugs generated the glutathionylated p53 with different kinetics. Thus, when the total p53 expression levels (assessed by direct Western

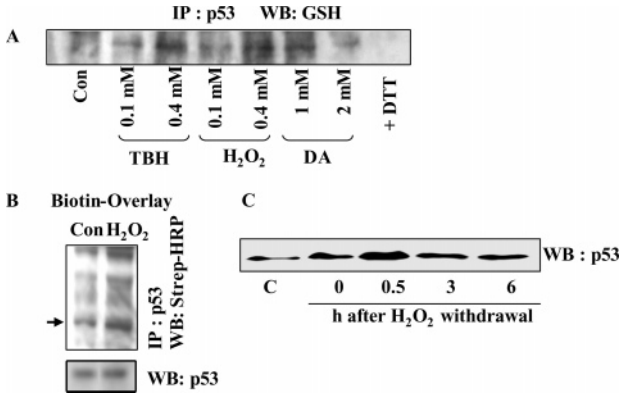

FIGURE 4: Oxidative stress increases levels of glutathionylated p53 in human tumor cells as determined by IP/Western, Biot-GST overlay, and glutathionylation susceptibility assays. (A) Oxidants increase the level of p53 glutathionylation in U87MG cells. Cells were treated with diamide (DA), H_2O_2, and TBH at the indicated concentrations for 15 min. p53 was immunoprecipitated, and the IPs were processed for Western analysis using GSH antibodies. In the last lane, p53 IP from 2 mM diamide-treated cells was exposed to 5 mM DTT before electrophoresis. (B) p53 immunoprecipitates from control and H_2O_2-treated (0.4 mM, 15 min) cells were electrophoresed, and the resulting blot was subjected to Biot-GST overlay assays. Arrow points to the glutathionylated p53 band. A direct Western blot of p53 is shown in the bottom panel. (C) Changes in the glutathionylation susceptibility of p53 after H_2O_2 and DNA-damaging treatments. U87MG cells were exposed to H_2O_2 (0.4 mM for 15 min) and further postincubated in oxidant-free medium for the indicated times. Equal protein amounts were then mixed with 0.1 mL of GSH-Sepharose beads (*31*). All of the bound proteins were eluted with 10 mM DTT, resolved by SDS−PAGE, and Western-blotted for p53.

analysis) were highest 10 h post-doxorubicin and post-m-AMSA treatments (Figure 3D, bottom panel), the level of thiolated p53 was at its lowest, and in case of vincristine, the levels of modified and unmodified p53 rose in parallel. Efforts were made to assess the extent of p53 glutathionylation in cells after DNA damaging and oxidative treatments described in this report; for this, we compared the band intensities of total p53 and glutathionylated p53 from a range of equivalent protein amounts in four separate experiments and quantitated the bands shifted by glutathionylation (see Figure 3A). These calculations showed that a maximum of 6−8% of p53 generated was thiolated during cell stress. The coexistence of glutathionated p53 with its unmodified form implies that a part of the p53 induced after DNA damage may remain inactive and that reversible S-thiolation may replenish active p53 as its biological transactions are pursued.

Exposure of Tumor Cells to Oxidants Induces p53 Glutathionylation. Because the extent of protein glutathionylation increases significantly after oxidative stress (*17*, *18*), we subjected the U87MG cells to acute oxidative stress by exposing them to moderate concentrations of H_2O_2, *tert*-butyl hydroperoxide (TBH), or diamide for 15 min and assessed the glutathionylation of the p53 protein. First, p53 IPs prepared from the oxidant-treated cells were electrophoresed, and the resulting Western blots were probed with antibodies to GSH. The acute oxidant stress resulted in a concentration-dependent increase in the level of glutathionylated p53 (Figure 4A). The oxidants used here have been shown previously to increase the extent of protein glutathionylation (*39*, *40*), which could occur through oxidation of reactive cysteines in proteins or oxidation of glutathione, and subsequent formation of mixed disulfides (*17*). In the second method, the blots containing the resolved p53 IPs were exposed to Biot-GST protein followed by Western analysis using Strep-HRP; this procedure confirmed the increased levels of modified p53 after H_2O_2 treatment (Figure 4B).

Changes in Glutathionylation Susceptibility of p53 Protein following the Exposure of Tumor Cells to Oxidizing Agents. Recently, we demonstrated that proteins with reactive cysteines can bind to immobilized glutathione matrices (GSH or GSSG) through disulfide bond formation in a reaction that mimics intracellular glutathionylation and that such a binding can reflect alterations in cysteine redox status for specific proteins (*31*). Therefore, we induced acute oxidative stress by exposing U87MG cells to 0.5 mM H_2O_2 for 15 min, and the cells were then postincubated in oxidant-free medium for up to 6 h. At each time point, equal amounts of protein (1 mg in cell extracts) were chromatographed on GSH-Sepharose, and the p53 protein levels present in the bound fractions (eluted by DTT) were assessed by Western analysis (*31*). p53 became markedly susceptible to glutathionylation 30 min after being treated with H_2O_2, which declined at later times (3 and 6 h), possibly due to intracellular dethiolation (Figure 4C). Both the early oxidation forms of p53 (sulfenic and sulfinic acids) and the glutathionylated p53 possess the ability to interact with GSH, and this may explain the increased level of binding of the p53 protein to the affinity matrix in H_2O_2-treated cells. Collectively, the data presented in Figures 3 and 4 reveal for the first time that p53 exists as a glutathionylated protein at low levels in cells; however, the degree of modification increases markedly after DNA damaging or oxidizing treatments.

Coexistence of Glutathionylation with Activating Phosphorylations in p53 Induced after DNA Damage. It is well-established that p53 induced by different stress stimuli is exquisitely modulated by various posttranslational modifications, including phosphorylation, acetylation, sumoylation, and others, most of which regulate the tumor suppressor in a positive manner so that it accomplishes its biological functions (*4*, *41*). To verify the presence of glutathionylation in activated p53, HCT116 cells were treated with CPT, and p53 isolated therefrom was assessed simultaneously for the presence of GSH, serine phosphorylations, and the target genes transactivated by p53. Immunoprecipitates of p53 protein prepared from these cells were Western-blotted in parallel using anti-p53 or anti-GSH antibodies. Figure 5A shows that p53 levels were increased as expected, and the level of GSH conjugation of the p53 was initially increased followed by a gradual decrease. p53 protein present in the same samples exhibited an increased level of phosphorylation at serine 20 and serine 392 (Figure 5B), both of which have been previously shown to accompany the DNA damage response (*42*, *43*). Further, the levels of $p21^{waf1}$, MDM2, and Bax proteins, whose gene transcription is well-known to be activated by p53 (*1*, *44*), were significantly elevated (Figure 5B). The studies performed in an identical setting suggest that p53, the level of which increased in response to DNA damage, was not only phosphorylated but also marginally glutathionylated, which constitutes a negative regulatory mechanism for the tumor suppressor.

Glutathionylated p53 Is Present in the Nuclei and Exhibits Inefficient Binding to DNA. Because p53 functions exclusively in nuclei, it was of interest to examine the subcellular

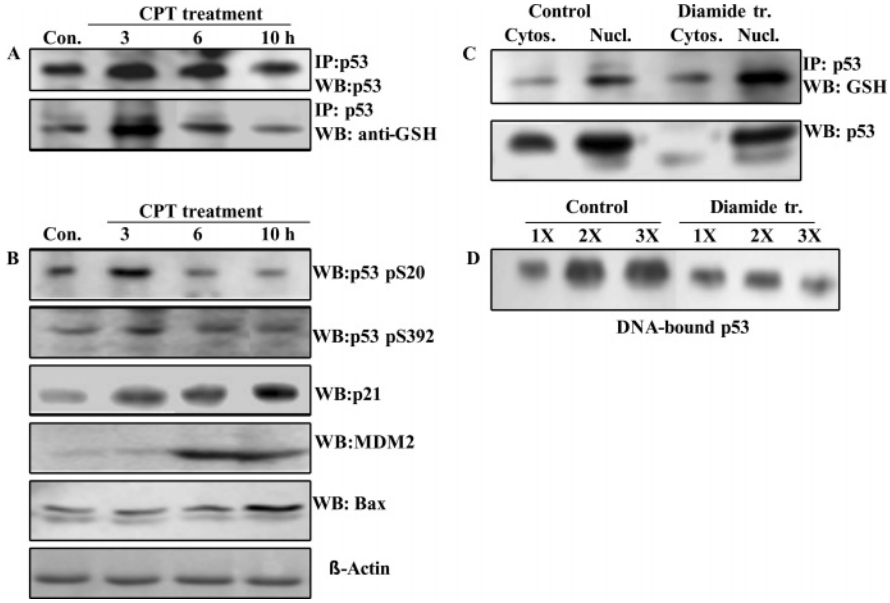

FIGURE 5: Glutathionylation coexists with the positive-regulatory phosphorylations in activated p53, where the modified protein is nuclear and functionally less active. (A) HCT116 cells were treated with 25 μM CPT for up to 10 h. At the specified times, p53 present in the cell extracts (300 μg in all samples) was immunoprecipitated. The IPs were electrophoresed on nonreducing SDS gels and blotted. Parallel blots were probed using anti-p53 or anti-GSH antibodies. The extracts used for IP were also resolved by SDS−PAGE and blotted. These blots were incubated with p53 phospho-specific antibodies (phosphoserine 20 and phosphoserine 392) or antibodies to hMDM2, p21^{waf1}, and human Bax proteins. The antigens were detected by routine Western blotting. (B) Localization of glutathionylated p53 in nuclei. HCT116 cells were treated with 1 mM diamide for 2 h. The cytosolic and nuclear fractions from control and diamide-treated cells were separated using an extraction kit. Equal protein amounts (300 μg) from these samples were subjected to immunoprecipitation of the p53 protein. The IPs were electrophoresed and Western-blotted using anti-GSH antibodies to obtain the pattern shown in the top panel. The levels of p53 in the cytosolic and nuclear fractions were assessed by direct Western blotting in the bottom panel. (C) Binding of p53 to its consensus recognition sequence in nuclear extracts from diamide-treated cells. HCT116 cells were treated with 1 mM diamide for 3 h. Nuclear extracts were prepared using the Pierce extraction kit. Binding of p53 to its recognition sequence in the presence of increasing levels of nuclear protein, 100 (1X), 200 (2X), and 300 μg (3X), was assessed by the DNA affinity immunoblotting (DAI) procedure as described in Materials and Methods.

location of the GSH-modified tumor suppressor. HCT116 cells were subjected to acute oxidative stress (1 mM diamide for 2 h), and the cytosolic and nuclear fractions were separated. p53 present in the extracts was immunoprecipitated, and Western blotting using antibodies to GSH was performed. The data in Figure 5C (top panel) clearly show that the level of nuclear p53 was slightly increased by diamide and it was glutathionylated. The bottom panel of Figure 5C displays the p53 levels assessed by direct Western blot analysis; the predominant nuclear location of p53 is again evident.

Next, the binding of p53 to its consensus recognition sequence in the nuclear extracts from control and diamide-treated HCT116 cells was assessed by the DAI procedure. While p53 from untreated controls showed a protein concentration-dependent increase in the level of DNA binding, its counterpart in diamide-treated cells showed a reduced level of DNA binding, which did not increase in the presence of additional nuclear protein (Figure 5D). We suggest that oxidation of p53 protein and its glutathionylation mediate this functional inactivation.

Ability of Glutathione-Enhancing Agents To Dethiolate Cellular p53 after DNA Damage. Proof of glutathionylation as a physiologically relevant mechanism requires the demonstration of its reversibility, and functional changes in its substrates in the cellular milieu. We sought to answer this question by inducing glutathionylation in p53 through DNA damage and then incubating the cells with cysteine prodrugs to increase the intracellular GSH content, and then examining the possible deglutathionylation of p53. The levels of p21^{waf1} protein, whose gene is transactivated by p53, were also assessed in this setting. *N*-Acetylcysteine (NAC) and glutathione ethyl ester (GEE) cell permeable nontoxic compounds rapidly elevate GSH levels in cells (*45*, *46*). In the first experiment, the HCT116 cells were exposed to CPT for 2 h and subsequently incubated in the presence or absence of NAC for 5 h. Figure 6A shows that p53 was significantly glutathionylated in response to CPT alone and lost ~50% of the modification when cells were incubated with NAC. Loss of glutathionylation was accompanied by a marginal but reproducible 30% increase in p21^{waf1} protein levels.

Similar experiments were performed to examine the dethiolation of p53 in the presence of GEE after tumor cell treatment with an oxidant or CPT (Figure 6B). The wild-type p53 present in HCT116 cells was slightly glutathionylated after oxidative stress induced by TBH and DNA damage by CPT, which were reduced by 50−75% in the presence of GEE. Again, the p21^{waf1} protein levels were slightly increased (10−40%) after deglutathionylation of p53 (Figure 6B). Cisplatin (cispt), a clinically used anticancer agent which damages DNA by platination and formation of intrastrand cross-links, induced a 3-fold increase in p53 levels and a discernible increase in the level of glutathionylation of p53 over untreated controls (Figure 6C). Incubation of cisplatin-treated cells with NAC reduced the level of glutathionylation of p53 to the levels found in untreated controls. Approximately 10% increased levels of p21waf1 protein accompanied the dethiolation of p53 in this setting. Col-

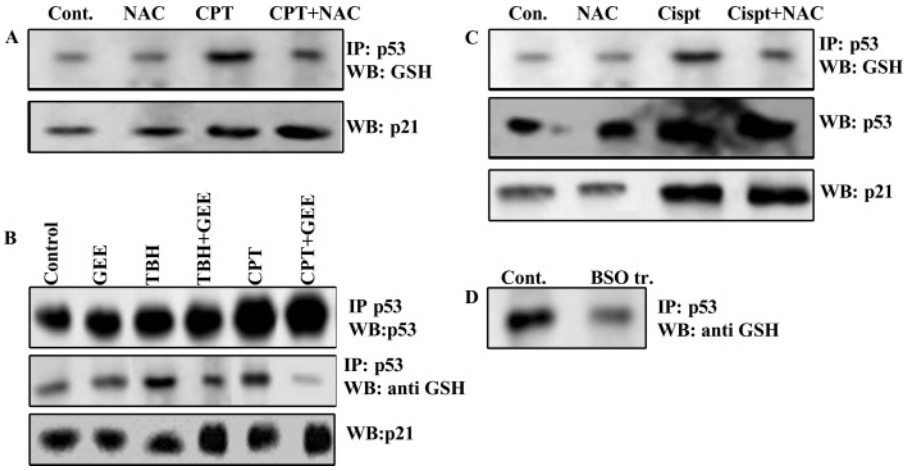

FIGURE 6: Augmentation of intracellular glutathione levels using *N*-acetylcysteine (NAC) or glutathione ethyl ester (GEE) results in the dethiolation of p53 in cells treated with DNA-damaging or -oxidizing agents. (A) HCT116 cells were exposed to 25 μM camptothecin for 2 h to induce p53 glutathionylation. These cells and untreated controls were washed and then incubated with 7.5 mM NAC (found to be optimal in separate experiments) for 5 h. p53 present in equivalent protein amounts (400 μg) was then immunoprecipitated and Western-blotted using antibodies to GSH. Cell extracts (50 μg) were immunoblotted in parallel for detection of $p21^{waf1}$ protein. (B) Following HCT116 cell treatment with *tert*-butyl hydroperoxide (TBH, 0.2 mM for 15 min) or camptothecin (CPT, 25 μM for 2 h), cells were washed and incubated with 4 mM GEE in the medium for 5 h. p53 immunoprecipitates prepared from cell extracts (400 μg of protein) were processed for Western blotting for the detection of p53 itself and glutathionylated p53. $p21^{waf1}$ protein levels were assessed by direct Western blotting. (C) Following cisplatin treatment (Cispt, 20 μM for 2 h), HCT116 cells were incubated in the presence or absence of 7.5 mM NAC for 5 h. Con. denotes untreated control cells. P53 immunoprecipitates were Western-blotted using GSH antibodies for detection of glutathionylated p53. Direct immunoblotting was performed so p53 and $p21^{waf1}$ protein levels could be determined. (D) Effect of GSH depletion on p53 glutathionylation. HCT116 cells were treated with buthionine sulfomine (BSO, 100 μM for 20 h). p53 immunoprecipitates from control and BSO-treated cells were Western-blotted using antibodies to GSH.

Table 1: Sequence and Elemental Composition of the p53 Glutathionylated Tryptic Peptides Identified by ESI-MS/MS

p53 peptide	peptide sequence[a]	elemental formula of the glutathione adduct	calculated monoisotopic peak	measured monoisotopic peak	error (ppm)
T6	^{121}SVT**C**TYSPALNK^{132}	$C_{65}H_{105}N_{17}O_{25}S_2$	794.8533	794.8671	17.3
T8	^{140}T**C**PVQLWVDSTPPPGTR^{156}	$C_{92}H_{143}N_{25}O_{31}S_2$	1070.999	1080.0212	20.5
T14	^{182}**C**SDSDGLAPPQHLIR^{196}	$C_{77}H_{124}N_{24}O_{29}S_2$	957.4282	957.4460	18.5

[a] The sequences of the GSH-modified tryptic peptides of p53 obtained from the in-gel digests are shown. The amino acid residue numbers corresponding to human p53 protein are shown in superscript. The modified cysteines are shown in bold.

lectively, the data presented in this section show that thiolation and dethiolation is a dynamic process for human p53 with potential to impact its functions.

Depletion of the Cellular Level of GSH Downregulates p53 Glutathionylation. Glutathione plays a key role in cellular defense response, and its reduction has been shown to both activate and suppress apoptotic stimuli (*47*). To gain insight into the redox signaling of p53 in the context of this study, we examined the effect of GSH deficiency on glutathionylation of p53. For this, HCT116 cells were exposed for 20 h to 50 μM buthionine sulfoximine (BSO), which lowers the cellular level of GSH by irreversibly inhibiting the rate-limiting enzyme γ-glutamylcysteine synthetase in its biosynthesis (*48*). Tumor cells retained approximately 10% of their GSH content compared to controls after this treatment (not shown). The steady-state glutathionylation of cellular p53 as determined by the immunoprecipitation of p53 followed by Western analysis using anti-GSH antibodies showed a marked reduction in BSO-treated cells (Figure 6D). A reduction of the level of GSH (and GSSG), each of which is a substrate for glutathionylation, may explain these results; however, depletion of the tripeptide is likely to generate oxidative stress signals, and more studies are required to determine the consequences of the decreased level of p53 glutathionylation in GSH-deficient cells.

Identification of Cysteines 124, 141, and 182 as the Sites of Glutathionylation in rp53 Protein by Mass Spectrometry. To obtain biochemical evidence of the identity of reactive cysteines that conjugate with GSH, we performed electrospray ionization tandem mass spectrometry (ESI-MS/MS). The p53 protein treated with GSH was run on nonreducing SDS gels, and the Coomassie-stained protein band was digested in gel with trypsin. A search of the MS/MS spectra against the NCBI protein database using MASCOT produced 11 matches to tryptic fragments of human p53, accounting for 43% of the protein sequence. Further examination of the peptide signals produced the identification of three tryptic p53 cysteine GSH conjugates. Table 1 displays the sequence of these peptides designated T6, T8, and T14, and their elemental composition. Cysteines 124, 141, and 182 were conjugated with GSH in peptides T6, T8, and T14, respectively. The isotopic distributions of these glutathionylated peptides are shown in Figure S2 of the Supporting Information. The masses, calculated and measured for these GSH-linked peptides, differed by only 20 ppm (Table 1).

To further confirm the identity of reactive cysteines that undergo glutathionylation in p53 protein, rp53 was treated with the SH alkylator biotinylated maleimide for 5 min for selective labeling of the exposed cysteines (*34*). The biotin-labeled peptides were purified from the tryptic digest, and the MALDI spectrum that was recorded exhibited a strong

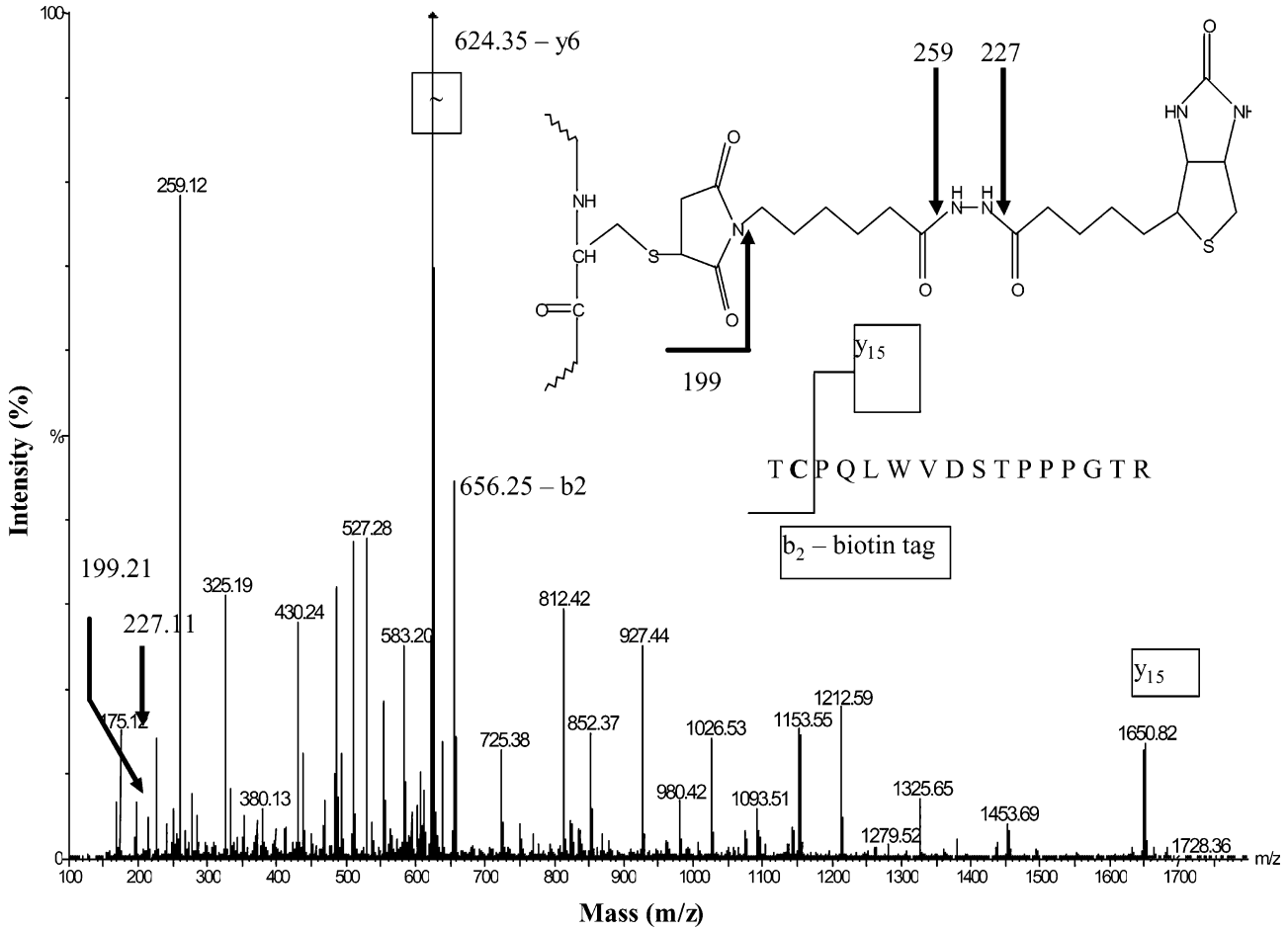

FIGURE 7: QTOF MS/MS spectrum of the T8 biotinylated peptide. rp53 was treated with biotin maleimide and trypsinized, and the biotin-containing peptides were purified on monomeric avidin resin (*32*). The doubly protonated molecular ion at *m*/*z* 1153.03 (T8 peptide of p53, ^{140}TCPVQLWVDSTPPPGTR^{156}) was fragmented in the collision cell of a QTOF instrument under low-energy conditions (42 eV). Three fragmentation ions (*m*/*z* 199.2, 227.1, and 259.1) indicate the presence of the biotin tag pictured in the inset. The presence of the y_{15} ion at *m*/*z* 1649.80 and a b_2 ion at *m*/*z* 656.25 containing the whole biotin maleimide tag locates the biotin tag on Cys141.

signal at *m*/*z* 2305.0867 (see Figure S3 of the Supporting Information), the sequence of which was identical to that of the T8 peptide, recorded earlier by ESI-MS/MS for the glutathionylated rp53 (Table 1). To accurately assess the biotin maleimide attachment to Cys141 found in this peptide, tandem mass spectrometry was performed after low-energy and high-energy CID fragmentation. The MS/MS fragmentation spectrum displayed in Figure 7 reveals the breakage pattern of this Cys-biotinylated peptide under low-energy CID conditions. The presence of the biotin tag is clearly indicated by the two abundant diagnostic ions at *m*/*z* 227.1 and 259.1. A prominent b_2 ion present at *m*/*z* 656.25 indicates that the biotin tag is located on the first two N-terminal amino acids; this notion is also confirmed by the presence of the y_{15} ion at *m*/*z* 1649.80. Fragmentation of the singly charged protonated molecular ion of the T8 peptide under high-energy CID conditions showed a modified y_{16} fragment ion containing a portion of the biotin maleimide tag with a mass of 199.1 Da (see Figure S4 of the Supporting Information). The cleavage of the biotin tag occurred simultaneously with the cleavage of the peptide backbone in this case. The results from the low- and high-energy CID MS/MS spectra unambiguously demonstrate the presence of the biotin probe on Cys141 from the T8 peptide of p53. Taken together, evidence obtained from ESI and MALDI mass spectrometry clearly proves that cysteines 124, 141, and 182 in human p53 are facile targets for GSH modification and Cys141 is probably the most reactive among them and, consequently, is likely to be highly prone to glutathionylation in cells.

Evidence that Glutathionylation Sites in Cellular p53 Are Likely To Be the Same as Those Found in Vitro. A majority of the reactive cysteines targeted for glutathionylation are located on the protein surface, possess lower pK_a values, and are readily accessible to solvents, oxidants, and sulfhydryl-reactive agents (*34*). Two approaches were undertaken to test whether the cysteines identified as sites of glutathionylation in the rp53 protein (Table 1 and Figure 7) represent the residues prone to this modification in cellular p53 as well. Cysteines 124, 141, and 182 identified by mass spectrometry have been confirmed as exposed residues by us (see Figure 9B) and others (*21*, *22*). The first approach involved the analysis of the protein microenvironment near these cysteines in the native crystal structure of human p53 (*36*). The reactivity of Cys residues within proteins is variable and depends on the local charge in the immediate vicinity, which determines their pK_a (*14*). The pK_a depends on the charge interactions of the thiol with the negatively charged side chains of nearby amino acids. We assessed the microenvironment of all seven cysteines present in the non-zinc-binding cluster in the DBD of the p53 crystal structure (Table 2). The results clearly show that cysteines 124, 141, and 182 which we identified as targets for glutathionylation are

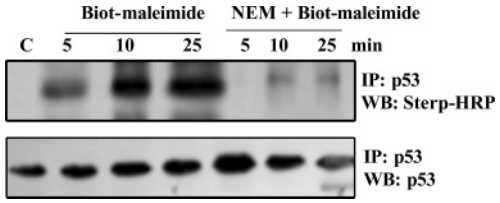

FIGURE 8: Rapid incorporation of biotin maleimide into cellular p53. Incorporationof biotin-labeled maleimide into the endogenous p53 protein in HCT116 cells was assessed as described in Materials and Methods. Briefly, HCT116 cell extracts were exposed to 5 mM Biot-maleimide with or without NEM pretreatment. NEM (5 mM) was also added to terminate the reactions. p53 immunoprecipitates were prepared from these extracts and Western-blotted using the Strep-HRP reagent.

located in the proximity of one or two charged residues, which is likely to impart a thiol anionic character to these cysteines. In contrast, the other cysteines which were not in a charged environment (Cys135 and -229) or whose charges were negated through salt bridge formation (Cys275) or hydrogen bonding with DNA (Cys277) were not detected as targets for GSH modification. Further, the presence of two charged residues, Lys139 and His233, near Cys141 validates its identity as probably the most reactive cysteine, borne out in our mass spectrometry studies.

Second, to gain further insight into the reactive cysteines in cellular p53, we studied the kinetics of incorporation of biotin maleimide into the cellular p53. The glutathionylatable reactive cysteines are generally located on protein surfaces and are solvent accessible; these thiols are readily alkylated by agents such as the biotinylated maleimide (*34*). Therefore, the extent of biotin maleimide incorporation is a good indicator of cysteine reactivity and, hence, a measure of glutathionylation potential. Therefore, we assessed the incorporation of the alkylator into the p53 protein. For this, dialyzed HCT116 cell extracts were exposed to biotin maleimide for 5−25 min in the presence or absence of 5 mM NEM, and the wild-type p53 present was analyzed by immunoprecipitation and Western blot analysis using Strep-HRP. Figure 8 shows a rapid incorporation of biotin maleimide into cellular p53, the kinetics of which are very similar to those of labeling of rp53 by Biot-GSSG observed in Figure 1A. These results, together with the association of a charged environment surrounding Cys124, -141, and -182 (Table 2), strongly suggest that the same cysteines are likely to be glutathionylation targets in the cellular p53 protein.

Protein Electrophoresis Reveals that Glutathionylation Inhibits p53 Oligomerization. Because Cys124 and -141 are located on the p53 surface, in the β-sheet behind the loop−sheet−helix (LSH) structure of p53 that contacts the DNA (refs *21* and *34* and Figure S1 of the Supporting Information), we surmised that glutathionylation of these residues may inhibit binding of p53 to DNA through structural perturbations and/or altering the protein oligomeric state. Therefore, we used glutaraldehyde to cross-link the rp53 protein that had been treated with GSH or left untreated. The samples were then resolved by SDS−PAGE. The gel stained with Coomassie blue shown in Figure 9A reveals that while untreated p53 was cross-linked in its oligomeric state by glutaraldehyde (lane 2), glutathionylated p53 failed to form these oligomers, after cross-linking (lanes 3 and 4). Exposure of the GSSG-treated rp53 to DTT prior to glutaraldehyde treatment restored the protein oligomerization (not shown). Since p53 in its native state exists and binds its target sequences as a tetramer (dimer of a dimer), these data suggest that conjugation of GSH to the reactive cysteines introduces structural perturbations that hinder the dimeric association of p53 protein. The data are also consistent with the reported inability of cysteine-oxidized p53 to form oligomers (*22*, *49*).

Simulation of Glutathionylation in the Crystal Structure of the p53−DNA Complex Demonstrates the Inhibition of DNA Binding and Disruption of Protein Dimerization. To gain a molecular and structural understanding by which glutathionylation inhibits binding of p53 to DNA, we bonded the GSH molecule to cysteines 124 and 141 in the crystal structure of the p53−DNA complex deduced by Cho et al. (*36*; PDB entry 1TSR). This structure has been used for modeling cancer mutations found in p53 and their DNA interactions (*50*) and validated recently for a study of p53 subunit interactions (*51*). It shows three copies of p53 monomers (A, B, and C) crystallized with the DNA consensus element. Of these, the A and B chains form a dimer as shown in Figure 9B and bind DNA, interacting with the major grooves in one turn of the duplex. Although there is some interaction between monomers B and C, the C monomer does not contact DNA. The DBD of monomer B (yellow ribbon in Figure 9B) makes several hydrogen bonds with the consensus site (GGGCA), with lysine 120 contacting the second guanine. Cys182, which we found to be a site for glutathionylation, is located in the H1 α-helix of the protein, faces away from the DBD in the crystal structure (Figure S1 and ref *34*), and is seen at the B−C dimer interface. Our modeling indicated that Cys182 modification will not affect the DNA binding with p53. Interestingly, Cys124 and Cys141, the two other sites for glutathionylation, lie in the proximity of the native structure of p53 at the dimer interface (marked in Figure 9B). Due to the spatial closeness of Cys124 and Cys141, it appears that only one of these residues can be modified by glutathionylation, but not both. Figure 9C shows the same interface in the crystal structure after a GSH molecule is linked with Cys124. Energy minimization showed that Cys124 modification not only inhibits the formation of the dimer but also distorts the loop containing Lys120 which normally interacts with DNA (see the displacement of the yellow monomer from DNA in Figure 9C). Therefore, interaction of p53 with DNA as well as the formation of the dimer from the monomers will not be possible after glutathionylation of Cys124. Identical structural impairment was observed after a GSH molecule is bridged to Cys141 in the p53 crystal structure, implying that thiolation of either of these reactive cysteines could alter p53 protein structure by blocking its oligomerization during oxidative stress. The protein modeling data together with different biochemical approaches described herein provide strong proof that structural alterations downregulate the p53 protein during the harmful condition that occurs when there is an excess of free radicals, a decrease in antioxidant levels, or both.

DISCUSSION

Despite the significant contributions of p53 to antioxidant mechanisms that control genetic stability (*52*), its transcription factor activity is highly prone to oxidative inactivation during physiological and pathological stresses that generate ROS and RON, and their byproducts, H_2O_2, and hydroxyl

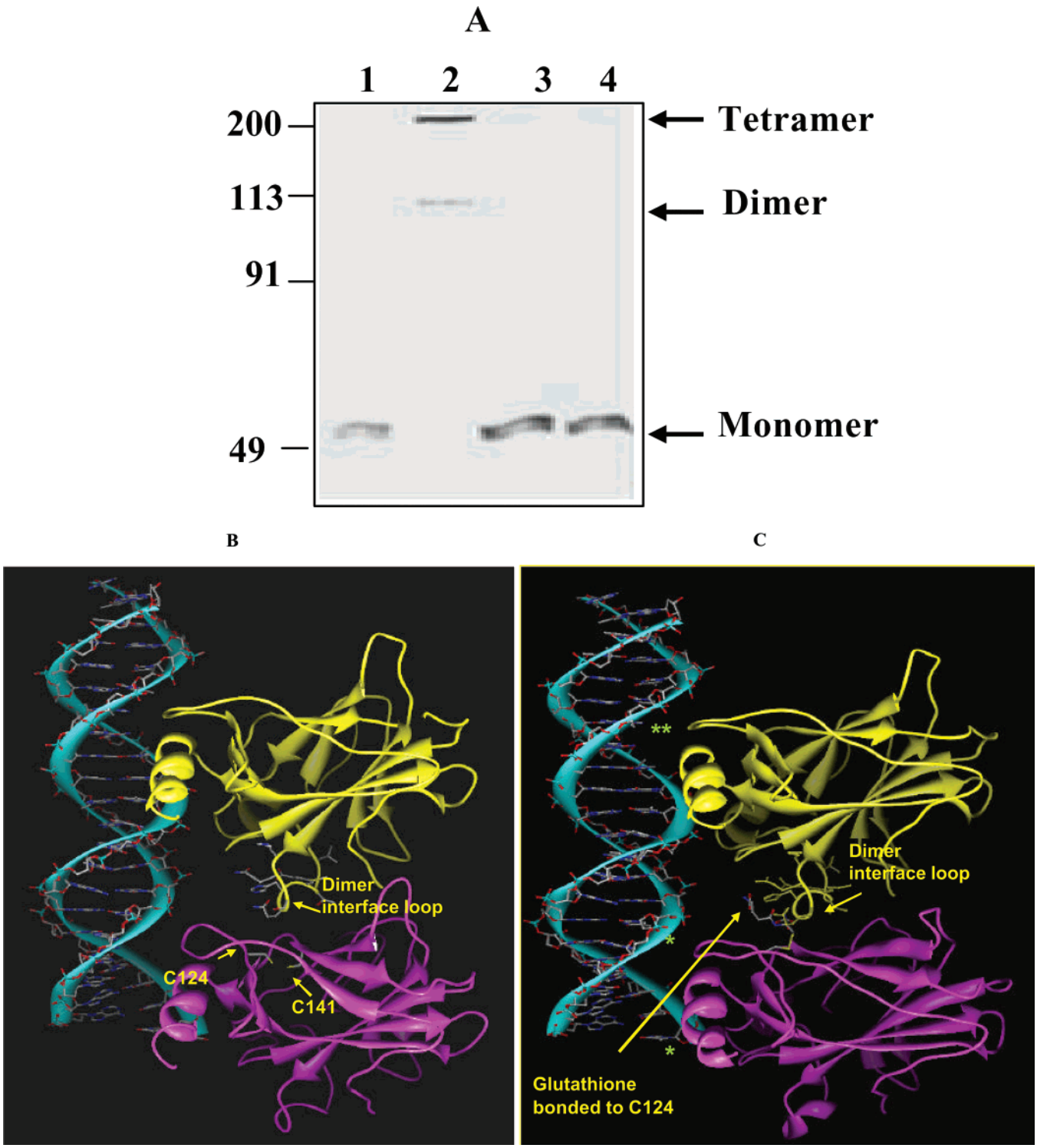

FIGURE 9: Protein cross-linking and structural modeling of S-glutathionylated p53. (A) Glutaraldehyde cross-linking and gel analysis of the oligomeric structure of glutathionylated p53. rp53 (5 μg) was treated with 5 mM GSH or GSSG for 1 h. The thiols present in the samples were removed by gel filtration on Bio-gel P6 spin columns. Glutaraldehyde was then added to the eluted proteins to a final concentration of 0.1% and the mixture incubated for 10 min. Next, SDS sample buffer containing 2-mercaptoethanol was added, and the samples were resolved by SDS−PAGE; the gel was then stained with Coomassie blue: lane 1, untreated rp53; lane 2, cross-linked rp53; lane 3, rp53 incubated with GSH, and then cross-linked; lane 4, rp53 incubated with GSSG, and then cross-linked. (B) Ribbon representation of the crystal structure of the p53−DNA complex. p53 chains A and B found in the crystal structure (PDB entry 1TSR) are colored magenta and yellow, respectively. These monomers form a dimer and stably associate with the consensus sequence in the crystal structure. Cys124 and Cys141 are present at the dimerization interface and are shown as color-coded balls and sticks. Note the proximity of these residues in the native structure. (C) Schematic ribbon representation of the energy-minimized model of p53 glutathionylated at Cys124. Procedures used for protein modeling are described in Materials and Methods. Structural alterations due to the modification resulted in the retraction of the DNA-presenting loop that harbors Lys120 in the B monomer (yellow, displaced loop marked with two asterisks). Changes also occurred at the dimer interface loop, and elsewhere in the molecule (some are marked with an asterisk). The deformation at the protein interface was determined to inhibit the dimerization. Modeling of a glutathione to Cys141 induced similar perturbations, and the spatial closeness of cysteines 124 and 141 indicated that both may not be thiolated in a single molecule.

Table 2: Microenvironment of the Non-Zinc-Binding Cluster of Cysteines in the p53−DNA Crystal Structure[a]

cysteine site	neighboring amino acid with positive charge	inter-residue distance (Å)	reactive Cys?[b]	other comments
Cys124	Lys139	7.3	yes	−
Cys135	−	−	no	no positively charged residues within 8 Å
Cys141	Lys139	6.3	yes	−
	His233	5.5		
Cys182	His178	4.1	yes	−
	His179	5.7		
Cys229	−	−	no	no positively charged residues within 10 Å
Cys275	Arg273	3.6	no	Arg273 forms a salt bridge with Asp281; therefore, it is likely to exert less influence on Cys275
Cys277	Arg280	4.1	no	Cys277 and Arg280 form one and two hydrogen bonds, respectively, with guanine in DNA; this will reduce the charge effects on Cys277

[a] The crystal structure of the p53−DNA complex (PDB entry 1TSR) was imported from the Protein Data Bank, and the native protein structure was visualized using the Argus Lab 4.0.1 molecular modeling and graphics program, which also allowed measurement of inter-residue distances. [b] Residues found to be reactive in this study. The microenvironment of zinc-binding cysteines 176, 238, and 242 was not examined as they may be less accessible for redox modifications.

radicals, which all arise as an inevitable consequence of aerobic metabolism. Additionally, the UV, γ-rays, hypoxia, chemotherapy drugs, and inflammatory cytokines contribute significantly to cellular oxidative stress and p53 modulation (*3*, *53*). This study provides the first and convincing evidence of the modification of specific cysteines by GSH conjugation in human p53 protein, and a molecular explanation for the resulting inhibition of the tumor suppressor after oxidative stress. Several lines of evidence show that p53 is subjected to glutathionylation, in vitro and in cells exposed to DNA-damaging agents, oxidants of endogenous (H_2O_2) and exogenous (diamide and TBH) origin. The results also show that glutathionylation has structural effects on p53 protein.

Significant levels of glutathionylation was observed for p53 at physiological thiol concentrations (Figure 1C), and this was stimulated by increased GSSG:GSH ratios in vitro, and oxidatively or nitrosatively stressed cells. While the augmentation of glutathionylated p53 in oxidant-treated cells was expected, its increase after DNA damage was intriguing and warrants discussion. Most of the posttranslational modifications that p53 accrues after genomic injury regulate it positively by increasing the transcriptional factor competency so that the check point functions are pursued appropriately. However, our results show that S-thiolation is a negative regulatory mechanism for p53, and it coexists with the positive regulatory phosphorylations. Further, the glutathionylated p53 was present in the nucleus, suggesting an important role in downregulation of its functional activities.

In our hands, the DNA-damaging anticancer drugs (CPT and cispt) at concentrations routinely used by researchers for p53 studies resulted in approximately 6−10% of the total p53 being glutathionylated. The modification reached much higher levels during oxidative stress. We suggest that p53 glutathionylation in vivo could be significant and may vary depending on the cell type, stress level, spatial considerations, nuclear microenvironment, and GSH abundance. The modified p53 (both recombinant and cellular) was less efficient in binding to DNA. Therefore, it appears that a small proportion of p53 generated in stressed cells becomes thiolated, remains inactive as a transcription factor, and coexists with the unthiolated active form. The molecular basis of p53 glutathionylation to divergent stimuli is currently unclear. However, given the paradigm that stress signals are transmitted to p53 by posttranslational modifications (*4*, *41*), we propose that p53 thiolation is an acute cellular response to various stresses, including genomic injury, redox imbalance, and other adverse stimuli. Like p53, the conserved cysteines in other transcription factors such as c-jun/AP-1, NF-κB, and Pax-8 also undergo glutathionylation, leading to their functional inactivation (*54*−*56*). With p53 being a key player in the expression of many proapoptotic genes (PUMA, Bax, etc.), it is tempting to speculate that inactivation of the tumor suppressor through glutathionylation may represent an acute adaptation strategy for suppressing the apoptotic signals generated in stressed cells. This defensive response may facilitate a reprogramming of gene expression for cytoprotection and/or prevent cell death (*57*, *58*). Further studies are required to test this hypothesis. Nevertheless, the glutathionated p53 may serve as a small pool of inactive suppressor protein, which could be drawn upon as the situation demands by conversion to a competent transcription factor through nonenzymatic or enzymatic dethiolation. Consistent with this notion, we found that p53 thiolation (following DNA damage or oxidant stress) can be reversed by increasing the intracellular GSH levels. The dethiolation of p53 achieved in the presence of NAC or GEE was accompanied by a modest increase in the level of $p21^{waf1}$ protein as well. The known interactions of p53 with the thiol exchange proteins (Ref-1 and thioredoxin reductase) (*12*, *13*) are also consistent with this premise. The negative regulation of p53 glutathionylation bears some analogy with the MDM2-p53 feedback loop (*2*), in which MDM2 transactivated by p53 functions to downregulate the tumor suppressor through ubiquitination-dependent proteolysis.

Human p53 possesses two clusters of cysteines in the DBD, which, interestingly, is devoid of any other posttranslational modifications. A striking feature of these cysteines is that they are all located in one area of p53 between the β-sandwich and the specific DNA-binding loops and helix (*19*). One cluster of three cysteines coordinates a zinc atom. The other cluster, harboring cysteines 124, 135, 141, and 277, is located adjacent to the zinc-binding site in or near the LSH region that makes contacts with DNA (refs *19* and *34* and Figure S1). The cysteines in the non-zinc-binding cluster are nicely positioned to modulate the access of the LSH region to the p53 recognition site. Of these, the cysteines at positions 124, 141, and 277 have been hypothesized previously to mediate the redox regulation of p53, in

particular because of their surface accessibility (*21*, *53*). In agreement, our mass spectrometry studies provided direct evidence of the site-specific glutathionylation of cysteines 124, 141, and 182 in the rp53 protein.

The protein cross-linking of glutathionylated p53 (Figure 9A) and molecular modeling studies (Figure 9B,C) provided new information about the core domain interactions and structural perturbations induced by glutathionylation for p53. A discussion of how p53 DBD interacts with DNA and contributes to the oligomerization of the protein is relevant in the context of our findings. p53 binds to DNA as a symmetrical tetramer consisting of two head-to-head (→← →←) dimers, with each dimer occupying a half-site of its recognition sequence (*59*). Although a single dimer is sufficient for DNA binding, interaction of the second dimer with the DNA dramatically enhances the binding affinity (>50-fold) and stabilizes the tetramer (*49*, *59*). This cooperative dimer−dimer interaction occurs even in the absence of the tetramerization domain (*36*, *60*, *51*), demonstrating the existence of an efficient core−core interaction, and this has been the subject of many studies (*60*−*62*). Evidence indicates that the p53−DBD species contributes significantly to the quaternary structure despite the fact that the tetramerization domain is structurally independent (*60*). For example, replacement of the p53 tetramerization domain with the dimerization domain of the GCN4 transcription factor bestows a near-wild-type p53 tumor suppression activity in vivo (*63*). Our studies with the p53−DNA crystal structure revealed for the first time that Cys124 and -141, present in a β-sheet just beneath the recognition loop, are at the dimer interface (Figure 9B,C and Figure S1). Further, the short H1 helix of p53 (Pro177−Cys182, the latter being a site of glutathionylaton), which resides near the zinc atom, has been shown to play an essential role in the intermolecular DBD dimerization; mutation of Cys182 (C182A) reduces the diffusion coefficient of complexation with consensus DNA (*60*, *61*). Interestingly, a previous study, based on theoretical considerations, hypothesized that Cys182 of p53 could be a target for glutathionylation (*22*). These authors, on the basis of molecular modeling, concluded that GSH conjugation with Cys182 would inhibit the dimerization of p53 (*22*). However, because Cys182 is juxtaposed with the recognition loop in the crystal structure, our studies did not support this possibility. Nevertheless, our data revealed that glutathionylation of either Cys124 or Cys141 could occur in a single p53 molecule, but not together due to their closeness and steric hindrance. The energy-minimized model of S-glutathionated p53 (at either Cys124 or Cys141) suggested that the modification would result in retraction of the recognition loop from DNA, and a dimer interface will not form. These data agree with the previous reports showing the failure of oxidized p53 to form tetramers (*22*, *49*) and provide a molecular explanation for inhibition of p53 function by S-thiolation. Our results hint that cysteines 124 and 141 play important roles in the core domain architecture of p53 and invite further structural studies for assessment of their contributions.

In summary, our observations shed light on new and understudied aspects of p53 redox regulation. The critical redox-sensitive cysteines in p53 were shown to reside in the proximal DNA-binding domain. In a reducing environment, these residues appear to organize the DBD and facilitate subunit interactions. However, when confronted by oxidative insult and other stresses, the reactive cysteines or their early oxidation products appear to be primed to undergo conjugation with GSH. While this modification may protect the critical and conserved cysteine residues of p53 (which are rarely mutated in human cancers) from irreversible oxidations, it also inhibits various p53 functions, albeit temporarily; the nonenzymatic and enzymatic thiol exchange mechanisms have the ability to reduce the mixed disulfide linkages and restore p53 function. Our results predict that a non-glutathionatable p53 protein may escape the redox regulation and may become more active than wild-type p53 in response to oxidative stress; consistent with this notion, the Cys141Arg mutation has been shown to be a dominant mutation for p53 (*64*), and the Cys124Ser mutation increases the level of DNA binding compared to that in wild-type p53 (*20*). Overall, the findings provide novel insight into the biochemical mechanisms that affect the p53 protein during cellular stress and possess clear relevance to different aspects of p53 in tumor biology, anticancer therapy and targeted chemoprevention. For example, whether a persistent S-thiolated state of p53 initiates oncogenic events, whether p53 mutant proteins are susceptible to glutathionylation, and whether S-thiolated p53 is a target for enhanced degradation are a few questions that emerge from this study.

ACKNOWLEDGMENT

We thank Dr. Jennifer Nyborg (Colorado State University) for the His-tagged p53 expression vector.

SUPPORTING INFORMATION AVAILABLE

Locations of cysteine residues in the three-dimensional ribbon structure of p53 protein (Figure S1), mass spectra of thiolated peptides from p53 (Figure S2), MALDI-TOF spectrum of the TCPVQLWVDSTPPPGTR peptide (T8) labeled with biotin maleimide (Figure S3), and MS/MS spectrum of the T8 peptide (biotin maleimide-conjugated molecular ion at *m*/*z* 2305.1 on the 4700 proteomics analyzer) (Figure S4). This material is available free of charge via the Internet at http://pubs.acs.org.

REFERENCES

1. Mills, A. A. (2005) p53: Link to the past bridge to the future, *Genes Dev. 19*, 2091−2099.
2. Inoue, T., Wu, L., Stuart, J., and Maki, C. G. (2005) Control of p53 nuclear accumulation in stressed cells, *FEBS Lett. 579*, 4978−4984.
3. Strosznajder, R. P., Jesko, H., Banasik, M., and Tanaka, S. (2005) Effects of p53 inhibitor on survival and death of cells subjected to oxidative stress, *J. Physiol. Pharmacol. 4*, 215−221.
4. Bode, A. M., and Dong, Z. (2004) Post-translational modification of p53 in tumorigenesis, *Nat. Rev. Cancer 4*, 793−805.
5. Martindale, J. L., and Holbrook, N. J. (2002) Cellular response to oxidative stress: Signaling for suicide and survival, *J. Cell. Physiol. 192*, 1−15.
6. Hainaut, P., and Milner, J. (1993) Redox modulation of p53 conformation and sequence-specific DNA binding in vitro, *Cancer Res. 53*, 4469−4473.
7. Verhaegh, G. W., Richard, M. J., and Hainaut, P. (1997) Regulation of p53 by metal ions and by antioxidants: Dithiocarbamate down-regulates p53 DNA-binding activity by increasing the intracellular level of copper, *Mol. Cell. Biol. 17*, 5699−5706.
8. Merwin, J. R., Mustacich, D. J., Pearson, G. D., and Merril, G. F. (2002) Reporter gene transactivation by human p53 is inhibited in thioredoxin reductase null yeast by a mechanism associated

with thioredoxin oxidation and independent of changes in the redox state of glutathione, *Carcinogenesis 23*, 1609−1615.
9. Hammond, E. M., and Giaccia, A. J. (2005) The role of p53 in hypoxia-induced apoptosis, *Biochem. Biophys. Res. Commun. 331*, 718−725.
10. Cobbs, C. S., Whisenhunt, T. R., Wesemann, D. R., Harkins, L. E., Van Meir, E. G., and Samanta, M. (2003) Inactivation of wild-type p53 protein function by reactive oxygen and nitrogen species in malignant glioma cells, *Cancer Res. 63*, 8670−8673.
11. Wu, H. H., Thomas, J. A., and Momand, J. (2000) p53 protein oxidation in cultured cells in response to pyrrolidine dithiocarbamate: A novel method for relating the amount of p53 oxidation in vivo to the regulation of p53-responsive genes, *Biochem. J. 351*, 87−93.
12. Hanson, S., Kim, E., and Deppert, W. (2005) Redox factor 1 (Ref-1) enhances specific DNA binding of p53 by promoting p53 tetramerization, *Oncogene 24*, 1641−1647.
13. Seemann, S., and Hainaut, P. (2005) Roles of thioredoxin reductase 1 and APE/Ref-1 in the control of basal p53 stability and activity, *Oncogene 24*, 3853−3863.
14. Claiborne, A., Mallett, T. C., Yeh, J. I., Luba, J., and Parsonage, D. (2001) Structural, redox, and mechanistic parameters for cysteine-sulfenic acid function in catalysis and regulation, *Adv. Protein Chem. 58*, 215−276.
15. Claiborne, A., Yeh, J. I., Mallett, T. C., Luba, J., Crane, E., Charrier, V. J., and Parsonage, D. (1999) Protein-sulfenic acids: Diverse roles for an unlikely player in enzyme catalysis and redox regulation, *Biochemistry 38*, 15407−15416.
16. Eaton, P., Jones, M. E., McGregor, E., Dunn, M. J., Leeds, N., Byers, H. L., Leung, K. Y., Ward, M. A., Pratt, J. R., and Shattock, M. J. (2003) Reversible cysteine-targeted oxidation of proteins during renal oxidative stress, *J. Am. Soc. Nephrol. 14*, S290−S296.
17. Klatt, P., and Lamas, S. (2000) Regulation of protein function by S-glutathiolation in response to oxidative and nitrosative stress, *Eur. J. Biochem. 267*, 4928−4944.
18. Ghezzi, P., Bonetto, V., and Fratelli, M. (2005) Thiol-disulfide balance: From the concept of oxidative stress to that of redox regulation, *Antioxid. Redox Signaling 7*, 964−972.
19. Rainwater, R., Parks, D., Anderson, M. E., Tegtmeyer, P., and Mann, K. (1995) Role of cysteine residues in regulation of p53 function, *Mol. Cell. Biol. 15*, 3892−3903.
20. Buzek, J., Latonen, L., Kurki, S., Peltonen, K., and Laiho, M. (2002) Redox state of tumor suppressor p53 regulates its sequence-specific DNA binding in DNA-damaged cells by cysteine 277, *Nucleic Acids Res. 30*, 2340−2348.
21. Hainaut, P., and Mann, K. (2001) Zinc binding and redox control of p53 structure and function, *Antioxid. Redox Signaling 3*, 611−623.
22. Sun, X. Z., Vinci, C., Makmura, L., Han, S., Tran, D., Nguyen, J., Hamann, M., Grazziani, S., Sheppard, S., Gutova, M., Zhou, F., Thomas, J., and Momand, J. (2003) Formation of disulfide bond in p53 correlates with inhibition of DNA binding and tetramerization, *Antioxid. Redox Signaling 5*, 655−665.
23. Srivenugopal, K. S., Shou, J., Mullapudi, S. R., Lang, F. F., Rao, J. S., and Ali-Osman, F. (2001) Enforced expression of wild-type p53 curtails the transcription of the O^6-methylguanine-DNA methyltransferase gene in human tumor cells and enhances their sensitivity to alkylating agents, *Clin. Cancer Res. 7*, 1398−1409.
24. Van Orden, K., Giebler, H. A., Lemasson, I., Gonzales, M., and Nyborg, J. K (1999) Binding of p53 to the KIX domain of CREB binding protein. A potential link to human T-cell leukemia virus, type I-associated leukemogenesis, *J. Biol. Chem. 274*, 26321−26328.
25. Mullapudi, S. R., Ali-Osman, F., Shou, J., and Srivenugopal, K. S. (2000) DNA repair protein O6-alkylguanine-DNA alkyltransferase is phosphorylated by two distinct and novel protein kinases in human brain tumour cells, *Biochem. J. 351*, 393−402.
26. Sullivan, D. M., Wehr, N. B., Fergusson, M. M., Levine, R. L., and Finkel, T. (2000) Identification of oxidant-sensitive proteins: TNF-α induces protein glutathiolation, *Biochemistry 39*, 11121−11128.
27. Cheng, G., Ikeda, Y., Iuchi, Y., and Fuji, J. (2005) Detection of S-glutathionylated proteins by glutathione S-transferase overlay, *Arch. Biochem. Biophys. 435*, 42−49.
28. Armstrong, R. N. (1997) Structure, catalytic mechanism, and evolution of the glutathione transferases, *Chem. Res. Toxicol. 10*, 2−18.
29. Listowsky, I. (2005) Proposed intracellular regulatory functions of glutathione transferases by recognition and binding to S-glutathiolated proteins, *J. Pept. Res. 65*, 42−46.
30. Liu, Y., Asch, H., and Kulesz-Martin, M. F. (2001) Functional quantification of DNA-binding proteins p53 and estrogen receptor in cells and tumor tissues by DNA affinity immunoblotting, *Cancer Res. 61*, 5402−5406.
31. Niture, S. K., Velu, C. S., Bailey, N. I., and Srivenugopal, K. S. (2005) S-Thiolation mimicry: Quantitative and kinetic analysis of redox status of protein cysteines by glutathione-affinity chromatography, *Arch. Biochem. Biophys. 444*, 174−184.
32. Schvchenko, A., Wilm, M., Vorm, M., and Mann, M. (1996) Mass spectrometric sequencing of proteins silver-stained polyacrylamide gels, *Anal. Chem. 68*, 850−858.
33. Perkins, D. N., Pappin, D. J., Creasy, D. M., and Cottrell, J. S. (1999) Probability-based protein identification by searching sequence databases using mass spectrometry data, *Electrophoresis 20*, 3551−3567.
34. Hamnell-Pamment, Y., Lind, C., Palmberg, C., Bergman, T., and Cotgreave, I. A. (2005) Determination of site-specificity of S-glutathionylated cellular proteins, *Biochem. Biophys. Res. Commun. 332*, 362−369.
35. Wen, B., Doneanu, C. E., Gartner, C. A., Roberts, A. G., Atkins, W. M., and Nelson, S. D. (2005) Fluorescent photoaffinity labeling of cytochrome P450 3A4 by lapachenole: Identification of modification sites by mass spectrometry, *Biochemistry 44*, 1833−1845.
36. Cho, Y., Gorina, S., Jeffrey, P. D., and Pavletich, N. P. (1994) Crystal structure of a p53 tumor suppressor-DNA complex: Understanding tumorigenic mutations, *Science 265*, 346−355.
37. Schonhoff, C. M., Daou, M. C., Jones, S. N., Schiffer, C. A., and Ross, A. H. (2002) Nitric oxide-mediated inhibition of Hdm2-p53 binding, *Biochemistry 41*, 13570−13574.
38. Sarangarajan, R., Apte, S. P., and Ugwu, S. O. (2006) Hypoxia-targeted bioreductive tyrosine kinase inhibitors with glutathione-depleting function, *Anticancer Drugs 17*, 21−24.
39. Wang, J., Boja, E. S., Tan, W., Tekle, E., Fales, H. M., English, S., Mieyal, J. J., and Chock, P. B. (2001) Reversible glutathionylation regulates actin polymerization in A431 cells, *J. Biol. Chem. 276*, 47763−47766.
40. Borges, C. R., Geddes, T., Watson, J. T., and Kuhn, D. M. (2002) Dopamine biosynthesis is regulated by S-glutathionylation. Potential mechanism of tyrosine hydroxylase inhibition during oxidative stress, *J. Biol. Chem. 277*, 48295−48302.
41. Xu, Y. (2003) Regulation of p53 responses by post-translational modifications, *Cell Death Differ. 10*, 400−403.
42. Shieh, S. Y., Taya, Y., and Prives, C. (1999) DNA damage-inducible phosphorylation of p53 at N-terminal sites including a novel site, Ser20, requires tetramerization, *EMBO J. 18*, 1815−1823.
43. Keller, D. M., and Lu, H. (2002) p53 serine 392 phosphorylation increases after UV through induction of the assembly of the CK2•hSPT16•SSRP1 complex, *J. Biol. Chem. 277*, 50206−50213.
44. Thornborrow, E. C., Patel, S., Mastropietro, A. E., Schwartzfarb, E. M., and Manfredi, J. J. (2002) A conserved intronic response element mediates direct p53-dependent transcriptional activation of both the human and murine bax genes, *Oncogene 21*, 990−999.
45. De Flora, S., Cesarone, C. F., Balansky, R. M., Albini, A., D'Agostini, F., Bennicelli, C., Bagnasco, M., Camoirano, A., Scatolini, L., Rovida, A., et al. (1995) Chemopreventive properties and mechanisms of N-acetylcysteine. The experimental background, *J. Cell. Biochem. 22* (Suppl.), 33−41.
46. Drake, J., Sultana, R., Aksenova, M., Calabrese, V., and Butterfield, D. A. (2003) Elevation of mitochondrial glutathione by γ-glutamylcysteine ethyl ester protects mitochondria against peroxynitrite-induced oxidative stress, *J. Neurocsi. Res. 74*, 917−927.
47. Sen, C. K. (2000) Cellular thiols and redox-regulated signal transduction, *Curr. Top. Cell. Regul. 36*, 1−30.
48. Bailey, H. H., Mulcahy, R. T., Tutsch, K. D., Arzoomanian, R. Z., Alberti, D., Tombes, M. B., Wilding, G., Pomplun, M., and Spriggs, D. R. (1994) Phase I clinical trial of intravenous L-buthionine sulfoximine and melphalan: An attempt at modulation of glutathione, *J. Clin. Oncol. 12*, 194−205.
49. Delphin, C., Cahen, P., Lawrence, J. J., and Baudier, J. (1994) Characterization of baculovirus recombinant wild-type p53.

Dimerization of p53 is required for high-affinity DNA binding and cysteine oxidation inhibits p53 DNA binding, *Eur. J. Biochem. 223*, 683−692.
50. Martin, A. C. R., Facchiano, A. M., Cuff, A. L., Hernandez-Boussard, T., Olivier, M., Hainaut, P., and Thornton, J. M. (2002) Integrating mutation data and structural analysis of the TP53 tumor-suppressor protein, *Hum. Mutat. 19*, 149−164.
51. Ma, B., Pan, Y., Gunasekaran, K., Venkataraghavan, R. B., Levine, A. J., and Nussinov, R. (2005) Comparison of the protein-protein interfaces in the p53-DNA crystal structures: Towards elucidation of the biological interface, *Proc. Natl. Acad. Sci. U.S.A. 102*, 3988−3993.
52. Sablina, A. A., Budanov, A. V., Ilyinskaya, G. V., Agapova, L. S., Kravchenko, J. E., and Chumakov, P. M. (2005) The antioxidant function of the p53 tumor suppressor, *Nat. Med. 11*, 1306−1313.
53. Wu, H. H., Sherman, M., Yuan, Y. C., and Momand, J. (1999) Direct redox modification of p53 protein: Potential sources of redox control and potential outcomes, *Gene Ther. Mol. Biol. 4*, 119−132.
54. Klatt, P., Molina, E. P., Lacoba, M. C. D., Padilla, C. A., Martinez-Galisteo, E., Barcena, J. A., and Lamas, S. (1999) Redox regulation of c-Jun DNA binding by reversible S-glutathiolation, *FASEB J. 13*, 1481−1490.
55. Pineda-Molina, E., Klatt, P., Vazquez, J., Marina, A., Lacoba, M. G. D., Perez-Sala, D., and Lamas, S. (2001) Glutathionylation of the p50 subunit of NF-κB: A mechanism for redox-induced inhibition of DNA binding, *Biochemistry 40*, 14134−14142.
56. Cao, X., Kambe, F., Lu, X., Kobayashi, N., Ohmori, S., and Seo, H. (2005) Glutathionylation of two cysteine residues in paired domain regulates DNA binding activity of Pax-8, *J. Biol. Chem. 280*, 25901−25906.
57. Dandrea, T., Bajak, E., Warngard, L., and Cotgreave, I. A. (2002) Protein S-glutathionylation correlates to selective stress gene expression and cytoprotection, *Arch. Biochem. Biophys. 406*, 241−252.
58. Winyard, P. G., Moody, C. J., and Jacob, C. (2005) Oxidative activation of antioxidant defence, *Trends Biochem. Sci. 22*, 207−210.
59. McLure, K. G., and Lee, P. W. K. (1998) How p53 binds DNA as a tetramer, *EMBO J. 17*, 3342−3350.
60. Ho, W. C., Fitzgerald, M. X., and Marmorstein, R. (2006) Structure of the p53 core domain dimer bound to DNA, *J. Biol. Chem. 281*, 20494−20502.
61. Dehner, A., and Kessler, H. (2006) Diffusion NMR spectroscopy: Folding and aggregation of domains in p53, *ChemBioChem 6*, 1550−1565.
62. Veprinstev, D. B., Freund, M. V., Andreeva, A., Rutledge, S. E., Tidow, H., Canadillas, J. M. P., Blair, C. M., and Fersht, A. R. (2006) Core domain interactions in full-length p53 in solution, *Proc. Natl. Acad. Sci. U.S.A. 103*, 2115−2119.
63. Pitenpol, J. A., Tokino, T., Thiagalingam, S., El-diery, W. S., Kinzler, K. W., and Vogelstein, B. (1994) Sequence-specific transcriptional activation is essential for growth suppression by p53, *Proc. Natl. Acad. Sci. U.S.A. 91*, 1998−2002.
64. Bischoff, J. R., Casso, D., and Beach, D. (1992) Human p53 inhibits growth in *Schizosaccharomyces pombe*, *Mol. Cell. Biol. 12*, 1405−1411.

BI700425Y